

Effects of disorder on quantum correlation of ultracold Bose gases released from a two-dimensional optical lattice

Yan Li* and Nao-Sheng Qiao

School of Physics and Electronics, Hunan University of Arts and Science, Changde 415000, China

Received 14 May 2012; Accepted (in revised version) 6 June 2012

Published Online 28 March 2013

Abstract. High-order quantum correlation provides powerful methods to reveal the quantum many-body behavior of ultracold atomic gases. In this work, the second-order quantum correlation is adopted to study the many-body behavior of ultracold Bose gases in the presence of both a two-dimensional optical lattice and weak disorder. According to investigations, it is found that even a weak disorder plays a significant role in the quantum many-body behavior, which manifests itself through the second-order quantum correlation. With the Bogoliubov theory, our studies show that both interatomic interactions and weak disorder would destroy the first-order quantum coherence of the condensate because of the depletion, and the resulting depletion has significant characteristic in the second-order correlation of the system.

PACS: 03.75.Hh, 03.75.Kk, 64.60.Cn

Key words: disorder, second-order correlation, ultracold atomic gases, optical lattice

1 Introduction

The high-order correlation was first used by Hanbury Brown and Twiss (HBT) to measure the size of a distant binary star [1]. Their pioneering experiment reveals that intensity fluctuations and resulting correlations contain information about the coherence and quantum statistics of probed system. This principle has found applications in many fields such as astronomy, high-energy physics, atomic physics, and condensed matter physics [2–5]. Recently, advances in atom cooling and detection have led to the observation of the atomic analog of the HBT effect [6, 7]. Henceforth the high-order correlation analysis becomes an increasingly important method for studies on complex quantum

*Corresponding author. *Email address:* liyan_2001@126.com (Y. Li)

phases of ultracold atoms. Correlation techniques have been successfully employed in recent experiments such as the atomic analog of the HBT effect [8], density-density correlation for degenerate bosonic and fermionic atomic gases in an optical lattice [9–11], second-order correlation of an atom laser [12], and the observation of pair-correlated fermionic atoms based on second-order correlation [13].

The high-order correlation for ultracold atomic gases released from an optical lattice has been intensively studied both experimentally and theoretically. Relevant experiments show that ultracold atoms, being prepared in a optical lattice and in a Mott-insulator state, display sharp peaks in their spatial correlation when released from the optical lattice [9,11]. These spatial correlation reveals the quantum statistics and the underlying order of bosonic or fermionic atoms in the optical lattices. In addition, the formalisms for describing the correlations observed between ultracold bosons released from an optical lattice have also been theoretically studied [14]. These formalisms, including the Bogoliubov method, the mean-field decoupling approach, and the particle-hole perturbative solution about the perfect Mott-insulator state are applicable for a broad range of behaviors in the lattice system and present numerous avenues for the future theoretical development.

On the other hand, physical effects driven by disorder in ultracold atom systems have become an active research field for many years [15]. As disorder is ubiquitous in nature and even only a weak disorder in quantum systems can have dramatic impact on the properties of the physical systems. Along this line, we theoretically investigate the problem of how weak disorder affects the second-order correlation of the ultracold Bose gas released from an optical lattice in the present paper. In the investigation, we mainly focus on the situation that the atoms are initially confined in a 2D optical lattice with weak quenched impurities and in a superfluid state. As is well known that the presence of external disorder leads to depletion in the ultracold Bose system [19,20]. Our results prove that the depletion due to the external disorder produces correlation and pairing lines in the (normalized) second-order correlation due to the classical correlation of the disorder. The correlation of disorder by itself is resulted from classical interference between random scattering routes, which is generally very complex and unusual [17]. According to our investigation, it is shown that the classical correlation of the disorder, even being switched off, can be displayed by the second-order correlation of the released ultracold atoms.

This paper is organized as follows. In Section II we give a general description of the Bose system in a 2D optical lattice with the presence of weak disorder. Section III derives the second-order correlation function for a simplified problem in which atoms are prepared in a 2D optical lattice with the presence of disorder and then freely expand. The details in the correlation function are examined in this section. A summary is provided in Section IV.

2 An ultracold Bose system in the presence of both a 2-D optical lattice and weak disorder

The many-body Hamiltonian for an ultracold Bose system in the presence of both a 2D optical lattice and weak disorder can be described as [16]

$$H - \mu N = \int d\mathbf{r} \psi^\dagger(\mathbf{r}) \left[-\frac{\hbar^2}{2m} \nabla^2 - \mu + V_0 \sum_{j=1}^2 \sin^2(kx_j) + V_{ran}(\mathbf{r}) + \frac{g}{2} \psi^\dagger(\mathbf{r}) \psi(\mathbf{r}) \right] \psi(\mathbf{r}), \quad (1)$$

where m and μ refer to the mass and the chemical potential of the bosons, respectively. $\psi(\mathbf{r})$ denotes the field operator for the Bose system, and $N = \int d\mathbf{r} \psi^\dagger(\mathbf{r}) \psi(\mathbf{r})$ represents the number operator of the Bose system. g is the coupling constant between the bosons. The lattice is taken to be simple square with $d = \pi/k$ and $b = 2k$ the length of the direct and reciprocal lattice vectors along each direction, where k is the wavelength of light used to produce the lattice. This lattice is of separable form, of the type produced in experiments with two sets of orthogonal counterpropagating light beams. The depth along each direction (i.e. V_0) is assumed to be the same.

In the above Hamiltonian, $V_{ran}(\mathbf{r})$ denotes the external disorder potential that brings disorder to the Bose system. The external disorder potential is here idealized as random distributions of hard-sphere potentials, which can be produced by a random potential associated with quenched impurities [18]

$$V_{ran}(\mathbf{r}) = \sum_{i=1}^{N_{imp}} v(\mathbf{r} - \mathbf{r}_i), \quad (2)$$

where \mathbf{r}_i ($i = 1, 2, \dots, N_{imp}$) stand for the randomly distributed positions of the impurities over the 2D optical lattice, and $v(\mathbf{r} - \mathbf{r}_i)$ represents the two-body interaction between the bosons and the impurity located at \mathbf{r}_i . N_{imp} denotes the total number of the quenched impurities. Regarding a dilute Bose system and small concentrations of the impurities, the potential $v(\mathbf{r} - \mathbf{r}_i)$ can be expressed by a pseudo-potential $v(\mathbf{r} - \mathbf{r}_i) = \tilde{g}_{imp} \delta(\mathbf{r} - \mathbf{r}_i)$, here \tilde{g}_{imp} is the effective coupling constant between the bosons and the quenched impurities. Thus, the Fourier transform of $V_{ran}(\mathbf{r})$ can be directly given by

$$V_{\mathbf{k}} = \frac{1}{V} \int e^{i\mathbf{k} \cdot \mathbf{r}} V_{ran}(\mathbf{r}) d\mathbf{r} = \frac{\tilde{g}_{imp}}{V} \sum_{j=1}^{N_{imp}} e^{i\mathbf{k} \cdot \mathbf{r}_j}, \quad (3)$$

where V is the total volume of the system. If the randomness is uniformly distributed with the density $n_{imp} = N_{imp}/V$ and Gaussian correlated, the three basic statistical properties of the disorder are given by

$$\overline{V_0} = \tilde{g}_{imp} n_{imp}, \quad (4)$$

$$\overline{V_{\mathbf{k}} V_{-\mathbf{k}}} = \tilde{g}_{imp}^2 n_{imp} / V, \quad (5)$$

$$\begin{aligned} \overline{V_{\mathbf{k}} V_{-\mathbf{k}} V_{\mathbf{p}} V_{-\mathbf{p}}} &= \left(\tilde{g}_{imp}^2 n_{imp} / V \right)^2 + \left(\tilde{g}_{imp}^2 n_{imp} / V \right)^2 \delta_{\mathbf{k}, \mathbf{p}} \\ &+ \left(\tilde{g}_{imp}^2 n_{imp} / V \right)^2 \delta_{\mathbf{k}, -\mathbf{p}}. \end{aligned} \quad (6)$$

Here the notation $\overline{\dots}$ refers to the ensemble average over all disorder configurations [17]. Eqs. (5) and (6) represent the first-order correlation and the second-order correlation of the disordered impurities, respectively. In order to calculate their values averaged over the realizations of the random potential, that is, over the positions of the scatterers, it is useful to note that most of the expanded terms in Eqs. (5) and (6) average to zero. The terms which contribute to the correlations are the ones for which the phases vanish. Specially, Eq. (6) is the result of the superpositions of two pairs of identical trajectories, those which have the same sequence of scattering events, either in the same or in the opposite directions. Later, we will prove that these correlations have impacts on the second-order correlation of the released bosonic gases.

Here, we restrict ourself to the condition that the chemical potential μ is smaller than the inter-band gap. Thereby, we can only consider the lowest band of the system. In the tight-binding approximation, the lowest Bloch band of the BEC system can be expressed in terms of Wannier functions as $\phi_{k_x}(x)\phi_{k_y}(y)$, where $\phi_{k_x}(x) = \sum_l e^{ilk_x} w_0(x - ld)$. Here the Wannier state $w_0(x)$ of the ground band can be approximated as a harmonic oscillator ground state

$$w_0(x) \approx \frac{1}{\pi^{1/4} \sigma^{1/2}} \exp\left(-\frac{x^2}{2\sigma^2}\right), \quad (7)$$

where σ denotes the oscillator length. The field operator can be expanded by the expression $\Psi(\mathbf{r}) = \sum_{\mathbf{k}} \hat{a}_{\mathbf{k}} \phi_{k_x}(x)\phi_{k_y}(y)$, where the annihilation operator $\hat{a}_{\mathbf{k}}$ represents eliminating a boson in the quasi-momentum basis $\hbar\mathbf{k} = \hbar(k_x, k_y)$ state.

On the basis of the above assumptions, the Bogoliubov approximation is still applicable and the Bogoliubov canonical transformation can be acquired as [16]

$$\hat{a}_{\mathbf{k}} = u_{\mathbf{k}} \hat{c}_{\mathbf{k}} - v_{\mathbf{k}} \hat{c}_{-\mathbf{k}}^\dagger - \frac{\sqrt{N_0} (u_{\mathbf{k}} - v_{\mathbf{k}})^2}{E_{\mathbf{k}}} V_{\mathbf{k}}, \quad (\mathbf{k} \neq 0) \quad (8)$$

with

$$\begin{aligned} u_{\mathbf{k}}^2 &= \frac{1}{2} \left(\frac{\varepsilon_{\mathbf{k}}^0 + n_0 U}{E_{\mathbf{k}}} + 1 \right), \quad v_{\mathbf{k}}^2 = \frac{1}{2} \left(\frac{E_{\mathbf{k}} + n_0 U}{E_{\mathbf{k}}} - 1 \right), \\ E_{\mathbf{k}} &= \sqrt{(\varepsilon_{\mathbf{k}}^0)^2 + 2n_0 U \varepsilon_{\mathbf{k}}^0}, \quad \varepsilon_{\mathbf{k}}^0 = 2J [2 - \cos(k_x d) - \cos(k_y d)]. \end{aligned} \quad (9)$$

Here the Bogoliubov quasiparticle operators $\hat{c}_{\mathbf{k}}$ is introduced, and N_0 denotes the total number of the particles in the condensate. J represents the tunnelling rate between neighboring wells, and U is an effective coupling constant. $n_0 = N_0 / (M \times M)$ ($M \times M$ is total number of the 2D lattice sites) is the average number of condensed atoms per lattice site. Specially, the last term in the Bogoliubov transformation (Eq. (8)) arises from the disorder, which corresponds to the physical process in which the disorder potential scatters a particle in the quasi-momentum state \mathbf{k} into the condensate.

When both the optical lattice and the external disorder potential are suddenly switched off, the atoms expand freely in the 2D space. In the far-field limit, after a free evolution of time t , the expanded field operator evolves to [14]

$$\Psi(\mathbf{r}, t) = \sum_{\mathbf{k}} \hat{a}_{\mathbf{k}} A(\mathbf{r}, t) F(\mathbf{Q}(\mathbf{r}) - \mathbf{k}), \quad (10)$$

where $\mathbf{Q}(\mathbf{r}) = m\mathbf{r} / (\hbar t) = (Q_x, Q_y)$ relates the 2D in situ momentum $\hbar\mathbf{Q}$ of the field to the final observation position $\mathbf{r} = (x, y)$.

$$A(\mathbf{r}, t) = \frac{\exp\left\{-\frac{\mathbf{r} \cdot \mathbf{r}}{2[W(t)]^2}\right\} \exp\left\{i\frac{\hbar\mathbf{Q}(\mathbf{r}) \cdot \mathbf{Q}(\mathbf{r})t}{2m}\right\} e^{i\theta}}{\left(\pi^{1/4}[W(t)]^{1/2}\right)^2} \quad (11)$$

is the common (complex) amplitude of all Wannier states. $W(t) = \sigma\sqrt{1 + (\hbar t / (m\sigma^2))^2}$ is the spatial width of the wave packets at time t and $\theta = \frac{1}{2}\arctan(\hbar t / (m\sigma^2))$. $F_M(\mathbf{Q})$ is defined as

$$F_M(\mathbf{Q}) = \frac{\sin(\frac{1}{2}M\mathbf{Q}_x d)}{\sqrt{M}\sin(\frac{1}{2}\mathbf{Q}_x d)} \frac{\sin(\frac{1}{2}M\mathbf{Q}_y d)}{\sqrt{M}\sin(\frac{1}{2}\mathbf{Q}_y d)}, \quad (12)$$

which is a peaked and periodic function. For M large enough, $F_M(\mathbf{Q})$ is sharply peaked at $\mathbf{Q} = (\mathbf{Q}_x, \mathbf{Q}_y) = (nb, mb)$ ($m, n = 0, \pm 1, \pm 2, \dots$) with peak height M .

For compactness of the following equations, we abbreviate our notation according to

$$F_M(\mathbf{Q}(\mathbf{r}_1) - \mathbf{q}) = F_{\mathbf{Q}_1 - \mathbf{q}}, \quad (13)$$

$$F_M(\mathbf{Q}(\mathbf{r}_2) - \mathbf{q}) = F_{\mathbf{Q}_2 - \mathbf{q}}, \quad (14)$$

and so on.

The normalized second-order correlation function for the released atoms is defined as

$$g^{(2)}(\mathbf{r}_1, \mathbf{r}_2, t) = \frac{G^{(2)}(\mathbf{r}_1, \mathbf{r}_2, t)}{\langle n(\mathbf{r}_1, t) \rangle \langle n(\mathbf{r}_2, t) \rangle}. \quad (15)$$

Here $G^{(2)}(\mathbf{r}_1, \mathbf{r}_2, t) = \langle \Psi^\dagger(\mathbf{r}_1, t) \Psi^\dagger(\mathbf{r}_2, t) \Psi(\mathbf{r}_2, t) \Psi(\mathbf{r}_1, t) \rangle$ represents the second-order correlation and $n(\mathbf{r}, t) = \Psi^\dagger(\mathbf{r}, t) \Psi(\mathbf{r}, t)$ is the density operator. $g^{(2)}(\mathbf{r}_1, \mathbf{r}_2, t)$ represents the joint

probability of detecting one particle at location \mathbf{r}_1 and another particle at location \mathbf{r}_2 at the same time t . $g^{(2)}(\mathbf{r}_1, \mathbf{r}_2) > 1$ (< 1) indicates a tendency of particle bunching (antibunching), typically for bosons (fermions).

Obviously, the first-order and the second-order correlation of the disorder (Eqs. (5 and 6)) should appear in the expansion of the second-order spatial correlation function for the released ultracold atoms. In Section IV, we will investigate the impact of the disorder on the second-order correlation for the released ultracold bosons in detail.

3 Depletion and second-order correlation for the released ultracold bosons

3.1 Depletion of the ultracold Bose system

When a Bose system is subject to the action of an external spatially random field, the condensate fraction reduces. Huang and Meng treated a Bose-condensed system in the case of asymptotically weak interatomic interaction and asymptotically weak disorder [20], and they suggested that there can exist the so-called Bose glass phase.

We consider the case of $T=0$ in our further investigations. In this case, the ground state of the system is the quasi-particle vacuum state, i.e., $\hat{c}_{\mathbf{k}}|vac\rangle = 0$. Thus the condensate population is reduced from the total number of atoms because of the depletion, i.e., $N_0 = N - \tilde{N}$, where $\tilde{N} = \sum_{\mathbf{q}} v_{\mathbf{q}}^2 + \sum_{\mathbf{q}} N_0 (u_{\mathbf{q}} - v_{\mathbf{q}})^4 \overline{V_{\mathbf{q}} V_{-\mathbf{q}}} / E_{\mathbf{q}}^2$ is the number of the depleted atoms.

Here the first term and the second term of \tilde{N} represent the quantum depletion due to the inter-atomic interaction and the depletion due to the scattering of condensed particles with the disorder potential, which are referred to the normal uncondensed and glassy component [19, 20], respectively.

For the convenience of the following numerical calculations and analyses, the disorder strength and the interaction strength are characterized by two dimensionless parameters:

$$\alpha = \frac{\overline{V_{\mathbf{k}} V_{-\mathbf{k}}}}{(2J)^2} = \frac{\tilde{g}_{imp}^2 n_{imp}}{V(2J)^2}, \quad (16)$$

and

$$\beta = \frac{U}{2J}, \quad (17)$$

respectively. The density of the released ultracold atomic gas $\rho(\mathbf{r}, t) = \overline{\Psi^\dagger(\mathbf{r}, t)\Psi(\mathbf{r}, t)}$ consists of two parts

$$\rho(\mathbf{r}, t) = \rho_0(\mathbf{r}, t) + \rho_1(\mathbf{r}, t), \quad (18)$$

the first term of which is the density of the condensed atoms

$$\rho_0(\mathbf{r}, t) = N_0 |A(\mathbf{r}, t)|^2 F_{\mathbf{Q}}^2, \quad (19)$$

and the second term is the density of the condensate depletion, which can be divided into two parts: $\rho_1(\mathbf{r}, t) = \rho_N(\mathbf{r}, t) + \rho_G(\mathbf{r}, t)$. Here

$$\rho_N(\mathbf{r}, t) = |A(\mathbf{r}, t)|^2 \sum_{\mathbf{q} \neq 0} v_{\mathbf{q}}^2 F_{\mathbf{Q}-\mathbf{q}}^2 \quad (20)$$

and

$$\rho_G(\mathbf{r}, t) = |A(\mathbf{r}, t)|^2 \sum_{\mathbf{q} \neq 0} R_{\mathbf{q}} F_{\mathbf{Q}-\mathbf{q}}^2 \quad (21)$$

represent the density of the normal uncondensed and the glassy component, respectively, where $R_{\mathbf{q}} = N_0 (u_{\mathbf{q}} - v_{\mathbf{q}})^4 \sqrt{V_{\mathbf{q}} V_{-\mathbf{q}}} / E_{\mathbf{q}}^2$. Fig. 1 (a-d) show the whole density profile of the ultracold bosonic gas, the density profile of the condensed atoms, the density profile of the normal uncondensed atoms and the density profile of the glassy component according to Eq. (19-21), respectively. In computing these density distributions, we consider 10,000

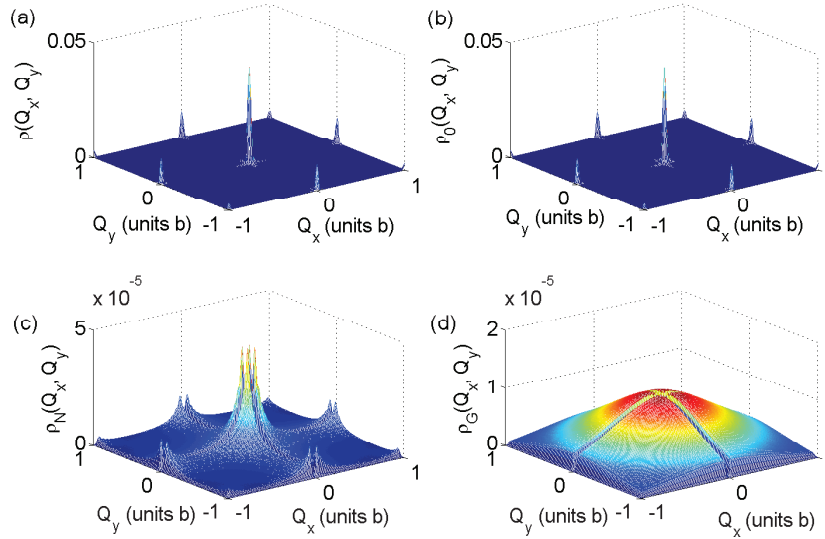


Figure 1: The density distribution of the released ultracold Bose gas: (a) The whole density of the ultracold Bose gas, (b) the density of the condensed atoms, (c) the density of the normal uncondensed atoms, and (d) the density of the glassy component. Here $(Q_x, Q_y) = (mx/(\hbar t), my/(\hbar t))$ are in units of $b = 2\pi/d$ (the length of the reciprocal lattice vector). Parameters: $N_0 = 10,000$ (the number of the condensed atoms), $d = 425$ nm (the spatial period of the optical lattice), $\sigma = 78$ nm (the oscillator length), $M = 25$ ($M \times M = 625$ is the total number of the 2D lattice sites), and $W(t) = 465$ μm (the spatial width of the wave packets). The disorder strength and the interaction strength related parameters are set as $\alpha = 1$ and $\beta = 2$ (which corresponds to a depletion fraction of 16% for the above parameters). Either the density of the depletion due to the inter-atomic interaction or the density of the depletion due to the disorder show splitting structure, which can be identified as a diffuse background in the time-of-flight images in practical experiments [21, 22].

Na atoms in the condensate and use $d = 425$ nm. Other related parameters are $\sigma = 78$ nm, $M = 25$, and $W(t) = 465$ μ m. And the disorder strength and the interaction strength related parameters are set as $\alpha = 1$ and $\beta = 2$ (which corresponds to a depletion fraction of 16%), respectively. Fig. 1 (c) and 1 (d) show that the density of the depletion, either due to the inter-atomic interaction or due to the disorder, has splitting structure. The condensed atoms compose the main part of the whole density, and the depletion is much smaller compared to the whole density for our parameters. Nevertheless the depleted fraction of a gaseous Bose-Einstein condensate in the optical lattice was directly observed as a diffuse background in the time-of-flight images [21, 22]. Those experimental measurements also prove that Bogoliubov theory provides a semiquantitative description even the depleted fractions is in excess of 50%.

3.2 Second-order correlation between the released Bosons

We now proceed to derive the second-order correlation function of the released atomic cloud. After being released from the combined potential of the optical lattice and the disorder potential, the second-order correlation of the ultracold atomic gas at time t can be easily calculated by applying the quasiparticle vacuum state to Eq. (15) and performing the ensemble average over all disorder configurations. According to the standard procedure and Eq. (4-6), it is obtained

$$\begin{aligned} \overline{G^{(2)}(\mathbf{r}_1, \mathbf{r}_2, t)} &= |A(\mathbf{r}_1, t)|^2 |A(\mathbf{r}_2, t)|^2 \{ [N_0^2 - N_0] F_{\mathbf{Q}_1}^2 F_{\mathbf{Q}_2}^2 \\ &+ \sum_{\mathbf{q} \neq 0} [N_0 (v_{\mathbf{q}}^2 + R_{\mathbf{q}})] (F_{\mathbf{Q}_1 - \mathbf{q}}^2 F_{\mathbf{Q}_2}^2 + F_{\mathbf{Q}_1}^2 F_{\mathbf{Q}_2 - \mathbf{q}}^2) \\ &+ \sum_{\mathbf{q} \neq 0, \mathbf{k} \neq 0} [v_{\mathbf{q}}^2 v_{\mathbf{k}}^2 + v_{\mathbf{q}}^2 R_{\mathbf{k}} + v_{\mathbf{k}}^2 R_{\mathbf{q}} + R_{\mathbf{k}} R_{\mathbf{q}}] F_{\mathbf{Q}_1 - \mathbf{k}}^2 F_{\mathbf{Q}_2 - \mathbf{q}}^2 \\ &+ \sum_{\mathbf{q} \neq 0} [v_{\mathbf{q}}^4 + 2v_{\mathbf{q}}^2 R_{\mathbf{q}} + R_{\mathbf{q}}^2] F_{\mathbf{Q}_1 - \mathbf{q}}^2 F_{\mathbf{Q}_2 - \mathbf{q}}^2 \\ &+ \sum_{\mathbf{q} \neq 0} [u_{\mathbf{q}}^2 v_{\mathbf{q}}^2 + 2u_{\mathbf{q}} v_{\mathbf{q}} R_{\mathbf{q}} + R_{\mathbf{q}}^2] F_{\mathbf{Q}_1 - \mathbf{q}}^2 F_{\mathbf{Q}_2 + \mathbf{q}}^2 \}. \end{aligned} \quad (22)$$

$\sum_{\mathbf{q}} F_M(\mathbf{Q}_1 - \mathbf{q}) F_M(\mathbf{Q}_2 \pm \mathbf{q}) = \sqrt{M} F_M(\mathbf{Q}_1 \pm \mathbf{Q}_2)$ and $F_M(\mathbf{Q} - \mathbf{q}) F_M(\mathbf{Q} - \mathbf{q}') \approx F_M(\mathbf{Q} - \mathbf{q})^2 \delta_{\mathbf{q}, \mathbf{q}'}$ are used in the above derivation, which can be easily derived and verified.

In the four-field correlation function, there are two terms that we should pay attention to: 1) $\sum_{\mathbf{q} \neq 0} [v_{\mathbf{q}}^4 + 2v_{\mathbf{q}}^2 R_{\mathbf{q}} + R_{\mathbf{q}}^2] F_{\mathbf{Q}_1 - \mathbf{q}}^2 F_{\mathbf{Q}_2 - \mathbf{q}}^2$ arises from the additional fluctuations due to the depletion, which has the same form as the depletion for the finite temperature ideal gas. Here, $v_{\mathbf{q}}^4$ arises from the quantum depletion due to the inter-atomic interaction, which is resulted from quantum many-body effect. Besides, $R_{\mathbf{q}}^2$ is the direct result of the second

term of Eq. (6), which represents additional fluctuation of the glassy component. In addition, $2v_q^2 R_q$ arises from the joint effect of the disorder and the inter-atomic interaction.

2) $\sum_{q \neq 0} \left[u_q^2 v_q^2 + 2u_q v_q R_q + R_q^2 \right] F_{Q_1-q}^2 F_{Q_2+q}^2$ arises from the process of physical scattering (both inter-atomic interaction and the disorder potential are the scatterers) and indicates the pairing between the particles with the opposite momentum owing to momentum conservations. $u_q^2 v_q^2$ results from the quantum depletion because of the inter-atomic interaction. Similar to the first term, R_q^2 is the direct result of the third term of Eq. (6), and the joint effect of the external disorder and the inter-atomic interaction accounts for the second term in the square bracket.

If there is no inter-atomic interaction, it is easy to deduce the second-order correlation for the released atoms with the sole effect of the disorder from Eq. (22)

$$\begin{aligned} \overline{G^{(2)}(\mathbf{r}_1, \mathbf{r}_2, t)} &= |A(\mathbf{r}_1, t)|^2 |A(\mathbf{r}_2, t)|^2 \{ [N_0^2 - N_0] F_{Q_1}^2 F_{Q_2}^2 \\ &+ \sum_{q \neq 0} N_0 R_q \left(F_{Q_1-q}^2 F_{Q_2}^2 + F_{Q_1}^2 F_{Q_2-q}^2 \right) \\ &+ \sum_{q \neq 0, k \neq 0} R_k R_q F_{Q_1-k}^2 F_{Q_2-q}^2 + \sum_{q \neq 0} R_q^2 F_{Q_1-q}^2 F_{Q_2-q}^2 \\ &+ \sum_{q \neq 0} R_q^2 F_{Q_1-q}^2 F_{Q_2+q}^2 \}. \end{aligned} \tag{23}$$

According to Eq. (23), it is shown that only the external disorder, even being switched off, can also lead to the depletion and pairing effect in the second-order correlation for the expanded ultracold atoms. Both Eq. (22) and Eq. (23) clearly show that the special classical correlations of the external disorder potential can be reflected by the second-order correlation of the released ultracold atoms.

In the following analyses, the correlation between two diagonal points will be discussed, i.e., $g^{(2)}(\mathbf{Q}_1, \mathbf{Q}_2)$ with $\mathbf{Q}_i = m\mathbf{r}_i / (\hbar t) = (Q_i, Q_i)$ ($i=1,2$). Since $F_M(\mathbf{Q})$ is sharply peaked at $\mathbf{Q} = (nb, mb)$ ($m, n = 0, \pm 1, \pm 2, \dots$), inspections of Eq. (18) and Eq. (22) generate

$$g^{(2)}(\mathbf{Q}_1, \mathbf{Q}_1) |_{Q_1=0} \simeq 1 - \frac{1}{N_0}, \tag{24}$$

$$g^{(2)}(\mathbf{Q}_1, \mathbf{Q}_1) |_{Q_1 \neq 0} \simeq 2, \tag{25}$$

$$g^{(2)}(\mathbf{Q}_1, -\mathbf{Q}_1) |_{Q_1 \neq 0} \simeq 1 + \left(\frac{u_{Q_1} v_{Q_1} + R_{Q_1}}{v_{Q_1}^2 + R_{Q_1}} \right)^2, \tag{26}$$

$$g^{(2)}(\mathbf{Q}_1, \mathbf{Q}_2) |_{Q_1 \neq Q_2, Q_1 \neq -Q_2} \simeq 1. \tag{27}$$

Here Eq. (25) and Eq. (26) are the manifestations of the correlation and the pairing terms in the four-field correlation. Besides these two special cases $g^{(2)}(\mathbf{Q}_1, \mathbf{Q}_2) \simeq 1$.

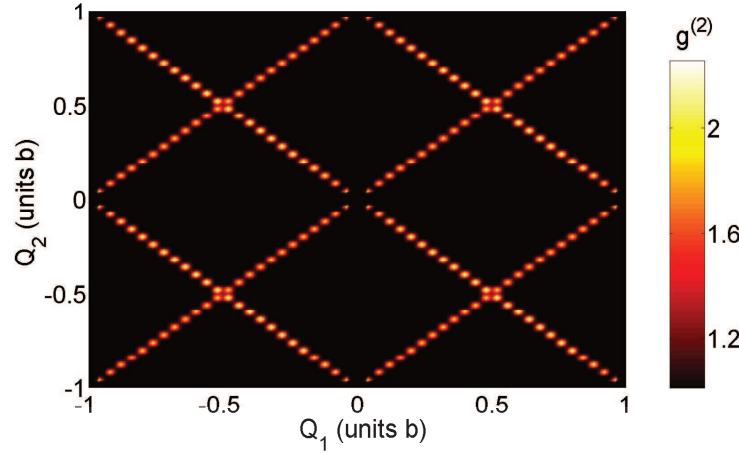


Figure 2: $g^{(2)}(\mathbf{Q}_1, \mathbf{Q}_2)$ with $\mathbf{Q}_i = m\mathbf{r}_i / (\hbar t) = (Q_i, Q_i)$ denotes a 2D diagonal vector. Q_i is in units of $b = 2\pi/d$ (the length of reciprocal lattice vector). All the parameters are kept the same as those in Fig. 1.

With the help of Eq. (18) and Eq. (23), $g^{(2)}(\mathbf{Q}_1, \mathbf{Q}_2)$ with the sole effect of disorder can be achieved, which is shown as follows

$$g^{(2)}(\mathbf{Q}_1, \mathbf{Q}_1) |_{Q_1=0} \simeq 1 - \frac{1}{N_0}, \quad (28)$$

$$g^{(2)}(\mathbf{Q}_1, \mathbf{Q}_1) |_{Q_1 \neq 0} \simeq 2, \quad (29)$$

$$g^{(2)}(\mathbf{Q}_1, -\mathbf{Q}_1) |_{Q_1 \neq 0} \simeq 2, \quad (30)$$

$$g^{(2)}(\mathbf{Q}_1, \mathbf{Q}_2) |_{Q_1 \neq Q_2, Q_1 \neq -Q_2} \simeq 1. \quad (31)$$

By carefully comparing Eq. (24-27) and Eq. (28-31), it is noted that the only difference of the normalized second-order correlations between these two different cases (one case with the combined effect of the inter-atomic interaction and the external disorder and the other case with the sole effect of the external disorder) lies in the correlations between atoms at opposite positions, i.e. $g^{(2)}(\mathbf{Q}_1, -\mathbf{Q}_1)$.

$g^{(2)}(\mathbf{Q}_1, \mathbf{Q}_2)$ is plotted in Fig. 2 with the disorder strength and the inter-atomic interaction strength related parameters set as $\alpha = 1$ and $\beta = 2$, respectively. Other related parameters are the same as those in the calculations of Fig. 1. In Fig. 2, the depletion and the pairing effects can be seen. The weak diagonal line (e.g. along $Q_1 = Q_2$) arises from the depletion, while the other diagonal line (e.g. along $Q_1 = -Q_2$) arises from the pairing between particles with opposite momenta. Additionally, it is found that the depletion line is weaker than the pairing line for our parameters.

Fig. 3 plots $g^{(2)}(\mathbf{Q}_1, \mathbf{Q}_2)$ with the sole effect of the disorder, i.e. with $\alpha \neq 0$ and $\beta = 0$. Other parameters are the same as the ones used in the above case. Fig. 3 clearly shows that both the depletion and the pairing line persist in this special case. Even the disorder

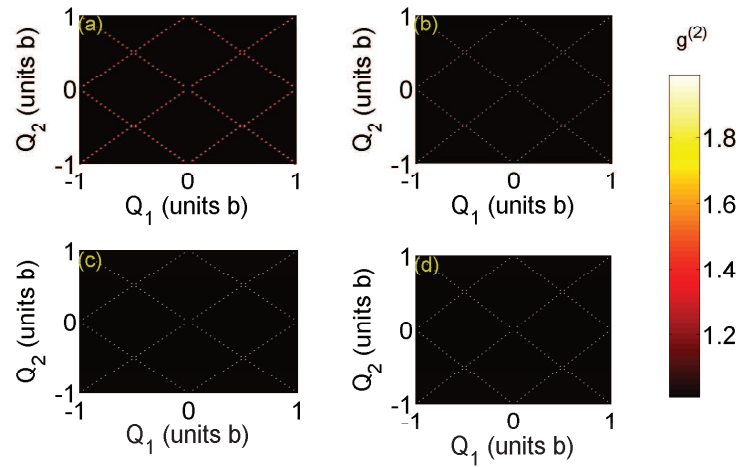


Figure 3: $g^{(2)}(\mathbf{Q}_1, \mathbf{Q}_2)$ without the effect of the inter-atomic interaction (i.e. $\beta=0$), and the disorder parameter α is set as (a) 1×10^{-6} , (b) 1×10^{-7} , (c) 1×10^{-8} , (d) 1×10^{-9} . Here $\mathbf{Q}_i = m\mathbf{r}_i / (\hbar t) = (Q_i, Q_i)$ denotes a 2D diagonal vector. Q_i is in units of $b = 2\pi/d$ (the length of the reciprocal lattice vector). Other parameters are the same as those in Fig. 1.

parameter α decreases to the level of 10^{-9} , the pairing and the depletion lines still exist. On the other hand, Fig. 3 also shows that the pairing line and the depletion line are approximately the same size in this situation.

Besides, according to Fig. 3, we observe that the bright spot along the correlation (pairing) line shrinks with the decrease of the disorder strength, which is disadvantageous to the experimental detection. Next, we will consider the effect of finite resolution of the detector on the measurement of density distribution. It is supposed that the finite

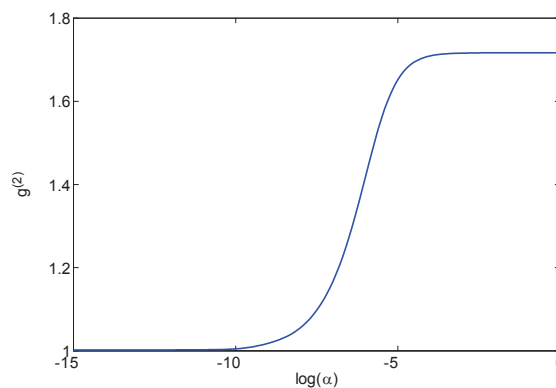


Figure 4: The second-order correlation $g^{(2)}(\mathbf{Q}_1, \mathbf{Q}_2)$ for $Q_1 = Q_2 = 13/25$ with the consideration of the finite resolution of the detector vs. the variation of the strength of the disorder. Here $\mathbf{Q}_i = m\mathbf{r}_i / (\hbar t) = (Q_i, Q_i)$ denotes a 2D diagonal vector. Q_i is in units of $b = 2\pi/d$ (the length of the reciprocal lattice vector). It is assumed that the finite width of the detector's pixel point is $5 \mu\text{m}$. Other related parameters are the same as those in Fig. 3.

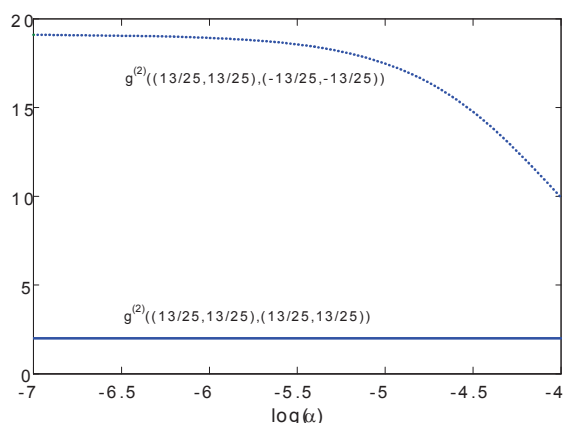


Figure 5: $g^{(2)}(\mathbf{Q}_1, \mathbf{Q}_1)$ (solid line) and $g^{(2)}(\mathbf{Q}_1, -\mathbf{Q}_1)$ (dashed line) for $Q_1 = 13/25$. Here $\mathbf{Q}_i = m\mathbf{r}_i / (\hbar t) = (Q_i, Q_i)$ denotes a 2D diagonal vector. Q_i is in units of $b = 2\pi/d$ (the length of the reciprocal lattice vector). During the numerical calculation, the interaction parameter β is fixed as 0.1 and the disorder parameter α ranges from 1×10^{-6} to 1×10^{-4} . Other related parameters are the same as those in Fig. 1.

width of the detector's pixel point is $5 \mu\text{m}$. By averaging the density over each whole pixel point of the detector, we can access the finite resolution effect on the second-order correlation. Fig. 4 presents the second-order correlation $g^{(2)}(\mathbf{Q}_1, \mathbf{Q}_2)$ for $Q_1 = Q_2 = 13/25$ (in units of b) with the consideration of the finite resolution of the detector. According to our evaluations, this special correlation becomes less observable as the disorder parameter decreases. Obviously in the practical experimental measurements, there is a limit to the strength of the disorder below which the correlation effect and the pairing effects caused by the weak disorder can not be observed.

On the contrary, when both the interaction parameter and the disorder parameter are zero, $g^{(2)}(\mathbf{Q}_1, \mathbf{Q}_2)$ reduces to $1 - \frac{1}{N_0}$ for any \mathbf{Q}_1 and \mathbf{Q}_2 . Clearly, there is no depletion or pairing effect developed when both the inter-atomic interaction and the disorder are suppressed. In the absence of both the inter-atomic interaction and the disorder, all of the atoms remain in the quasi-momentum state $\hbar\mathbf{k} = 0$ and form a coherent condensate. Therefore the depletion and pairing line can not form in the spatial second-order correlation without the scattering between the ultracold atoms.

In Fig. 5, when the interaction parameter β is fixed as 0.1 and the disorder parameter α ranges from 10^{-7} to 10^{-4} , we compares closely $g^{(2)}(\mathbf{Q}_1, \mathbf{Q}_2)$ for $Q_1 = Q_2 = 13/25$ (along the diagonal line $Q_1 = Q_2$, in units of b) with $g^{(2)}(\mathbf{Q}_1, \mathbf{Q}_2)$ for $Q_1 = -Q_2 = 13/25$ (along the diagonal line $Q_1 = -Q_2$, in units of b). Other parameters are kept the same as the ones used in the numerical calculation of Fig. 2. This figure shows that the value of the normalized second-order correlation along the depletion line always equals to 2 even when the disorder parameter varies, which can be verified by Eq. (25). However the value of the normalized second-order correlation along the pairing line is observed to decrease as strength of the disorder increases, which can also be understood with the help of Eq. (26).

4 Conclusions

In summary, the second-order correlation of the ultracold atoms released from a 2D optical lattice potential in the presence of weak disorder is analytically investigated within the framework of Bogoliubov theory. A general description of the ultracold Bose system and the Bogoliubov transformation for the bosons in the 2D optical lattice with weak disorder are first outlined. Then we applied the Bogoliubov transformation to the investigation of the second-order correlation function for the released ultracold atoms. When the atoms are initially confined in the combined potential (the optical lattice and the additional disorder potential) and in a superfluid state, the quantum tunneling between two consecutive wells can still ensure full coherence even in the presence of weak disorder and the separated wells created by the optical lattice. As a result, the Bogoliubov approximation is still applicable in this situation [16], and the Bogoliubov method provides us with a concise context, in which we can discuss the second-order correlation of the system. Thereby the role the disorder plays in the second-order correlation is distinct in our analyses.

Being similar to the role that the inter-atomic interaction plays in the second-order correlation for the released bosonic gases [14], the disorder produce pairing and correlation effects in the second-order correlation of the ultra-cold atoms when released from the optical lattice. Even with the inter-atomic interaction being excepted, the depletion and the pairing effects persist with the sole effect of the external disorder potential. By contrast, the depletion and the pairing structure cannot form when both the inter-atomic interaction and the disorder are absent. We derived the properties of the depletion and the pairing effects in detail, where different settings of the strength of the inter-atomic interaction and the disorder were specially considered in the investigations.

From our investigations, it is also noticed that the form of the second-order correlation due to the disorder is somewhat similar to the form of the second-order correlation due to the inter-atomic interaction. However they are the consequences of different physical process: The second-order correlation due to the disorder is caused by special interference of certain random scattering routes, while the second-order correlation due to the inter-atomic interaction is the result of quantum many-body effect. Although these two effects show similar functional behaviors in the second-order correlation for the released ultracold atoms, they display pure classical effect and quantum effect, respectively.

Acknowledgments We are grateful to the invaluable discussions with Prof. H. W. Xiong. This work is sponsored by the doctoral initiating project of Hunan University of Arts and Science.

References

- [1] R. H. Brown and R. Q. Twiss, *Nature (London)* 177 (1956) 27.
- [2] L. Mandel and E. Wolf, *Optical Coherence and Quantum Optics* (Cambridge University Press, Cambridge, 1995).

- [3] M. O. Scully and M. S. Zubairy, *Quantum Optics* (Cambridge University Press, Cambridge, 1997).
- [4] G. Baym, *Acta Phys. Pol. B* 29 (1998) 1839.
- [5] D. H. Boal, C. K. Gelbke, and B. K. Jennings, *Rev. Mod. Phys.* 62 (1990) 553.
- [6] M. Yasuda and F. Shimizu, *Phys. Rev. Lett.* 77 (1996) 3090.
- [7] R. Bach and K. Rzazewski, *Phys. Rev. A* 70 (2004) 063622.
- [8] M. Schellekens, R. Hoppeler, A. Perrin, J. Viana Gomes, D. Boiron, A. Aspect, and C. I. Westbrook, *Science* 310 (2005) 648.
- [9] S. Föling, F. Gerbier, A. Widera, O. Mandel, T. Gericke, and I. Bloch, *Nature (London)* 434 (2005) 481.
- [10] W. D. Phillips and J. V. Porto, *Phys. Rev. Lett.* 98 (2007) 080404.
- [11] T. Rom, Th. Best, D. van Oosten, U. Schneider, S. Fölling, B. Paredes, and I. Bloch, *Nature (London)* 444 (2006) 733.
- [12] A. Öttl, S. Ritter, M. Köhl, and T. Esslinger, *Phys. Rev. Lett.* 95 (2005) 090404.
- [13] M. Greiner, C. A. Regal, J. T. Stewart, and D. S. Jin, *Phys. Rev. Lett.* 94 (2005) 110401.
- [14] E. Toth, A. M. Rey, and P. B. Blakie, *Phys. Rev. A* 78 (2008) 013627.
- [15] J. E. Lye, L. Fallani, M. Modugno, D. S. Wiersma, C. Fort, and M. Inguscio, *Phys. Rev. Lett.* 95 (2005) 070401; L. Sanchez-Palencia, D. Clement, P. Lugan, P. Bouyer, G. V. Shlyapnikov, and A. Aspect, *Phys. Rev. Lett.* 98 (2007) 210401 (2007).
- [16] Y. Hu, Z. Liang, and B. Hu, *Phys. Rev. A* 80 (2009) 043629.
- [17] E. Akkermans and G. Montambaux, *Mesoscopic Physics of Electrons and Photons* (Cambridge University Press, Cambridge, 2007).
- [18] G. E. Astrakharchik, J. Boronat, J. Casulleras, and S. Giorgini, *Phys. Rev. A* 66 (2002) 023603.
- [19] V. I. Yukalov and E. P. Yukalova, *Phys. Rev. A* 74 (2006) 063623.
- [20] K. Huang and H. Meng, *Phys. Rev. Lett.* 69 (1992) 644.
- [21] K. Xu, Y. Liu, D. E. Miller, J. K. Chin, W. Setiawan, and W. Ketterle, *Phys. Rev. Lett.* 96 (2006) 180405.
- [22] B. Lu, X. Tan, B. Wang, L. Cao, and H. Xiong, *Phys. Rev. A* 82 (2010) 053629.